CPQ Orthopaedics (2019) 3:2
Research Article

WNT3A Regulates Osteogenic Differentiation of Periosteum Cells in HA/TCP Matrix

Diwei Wu[1#], Shaoyu Liang[1#], Xuanhe You[1#], Jiazhuang Xu[2*] & Shishu Huang[1*]

[1]*Department of Orthopedic Surgery, West China Hospital, Sichuan University, Chengdu, China*

[2]*College of Polymer Science and Engineering and State Key Laboratory of Polymer Materials Engineering, Sichuan University, Chengdu, China*

# Authors have equal contribution

[*]**Correspondence to:** Dr. Shishu Huang & Jiazhuang Xu, Department of Orthopedic Surgery, West China Hospital & College of Polymer Science and Engineering and State Key Laboratory of Polymer Materials Engineering, Sichuan University, Chengdu, China.

Copyright

Received: 06 May 2019

Published: 15 May 2019

Keywords: *HA/TCP Matrix; Periosteal Cells; Bone Engineering; Cytometry Analysis*

Abstract

Periosteal cells are a heterogeneous population that has a potential of osteogenic differentiation. It is still a challenge that their osteogenetic capacity *in vivo* is not efficient. We hypothesize that Wnt3a, one of the Wnt family in the regulation of osteogenesis, enhances bone formation *in vivo* and has the potential treatment in bone defect. Herein, a population of Wnt3a over-expressed periosteum cells was generated in the treatment of calvarial defect mouse model. Periosteal cells were primarily harvested from GFP mice and transfected with Wnt3a lenti-virus (MOI=1). The Wnt3a positive periosteal cells were seeded into a biodegradable scaffold (beta-tricalcium phosphate) and implanted into calvarial defect (5mm in diameter) mouse model. After two months transplantation, we used H&E, Masson and micro-CT to evaluate the bone formation *in vivo*. Compared to control and blank group, new bone formation was observed in Wnt3a over-expressed group that is the lamellar bone. Additionally, the cell and scaffold mix was detected by micro-CT and the Wnt3a over-

expressed group significantly generated higher volume, more bone trabecular and lower trabecular space in new bone. Wnt3a promotes osteogenesis *in vivo* and the periosteal cell is one of the seed cells that can be used in the treatment of bone defect combined with tissue engineering and cell therapy.

Introduction

Bone engineering has been considered as one of the most important strategies in bone regeneration. The generation of new bone is aimed to replace or restore the dysfunctional or damaged bone. This meets the need of clinical and socio-economic interests [1]. Combination of cells, scaffolds, and appropriate growth factors is one of the methods in the regeneration of bone defects. These factors include BMPs, FGFs, VEGFs, IGFs, TGF-beta, PDGF, PTH/PTHrP, etc. Up to date, the generation of new bone has not yet been efficient and it requires further optimization [2]. In particular, Wnt3a, as one of the growth factors, has been highlighted in the involvement of bone development and generation. However, the role of Wnt3a in bone regeneration is still not clear.

Periosteal cells are a heterogeneous population that has a potential of osteogenic differentiation, which contains osteogenitor cells [3-5]. Periostem cells have been reported to regenerate bone defects, which are believed to mimick periostem for bone repair [3-5]. However, Seeding periosteum cells for bone issue engineering is a challenge that the osteogenetic capacity *in vivo* is still not efficient. HA/TCP matrix is regarded as one the promising materials in bone replenish [6,7]. It has been reported to be osteogenic induction [6,7]. Wnt family proteins are generally involved in the regulation of vertebrate skeletal development and bone homeostasis [8,9] Wnt3a, one of the nineteen members, was identified as a key factor in the development of long bones. Wnt3a was associated with Wnt4 and Wnt14 to activate the canonical Wnt signaling pathway in the developing synovial joints [10].

In this study, we hypothesize that Wnt3a enhances new bone generation *in vivo* and has a potential treatment in bone defect. A population of Wnt3a over-expressed (Wnt3a OE) periosteum cells was generated and implanted in a calvarial defect mouse model [6]. Compared to periosteum cells, osteogenesis *in vivo* was increased in Wnt3a OE periosteum cells that were confirmed by Masson and micro-CT. This has further been used in the treatment of the calvarial defect mouse model that suggested a new bone formation was enhanced by the Wnt3a modulation. Together with tissue engineering and cell therapy, this study may shed new lights on bone regeneration.

Methods and Material

Cell Culture

All animal experiments were approval by the Institutional Animal Care and Use Committee, Shenzhen People Hospital, Jinan University. The Green Fluorescent Protein (GFP) mice (C57BL/6-Tg(UBC-GFP)30Scha/J) and C57 mice (4-week-old, 15~20g weight, male) were purchased from Dashuo laboratory animal Co., Ltd. The periosteal cells were harvested by enzyme digestion (contained 3mg/ml Collagenase Type I and 4mg/ml dispase) and cultured in minima essential medium (MEM) supplemented with 20%

fetal bovine serum (FBS). The primary cells were cultured for 14 days before transfection and seeded in the density of 10 cells/cm^2.

Flow Cytometry Analysis

The GFP periosteal cells were trypsinized and washed with PBS twice. These cells were mixed with1ml cold 4-Phenylbutyric acid (PBA) and centrifuged. Subsequently, cells were mixed with antibodys (1 ul CD105-647Flour, 1ul Scal-1-PE, 1ul CD34-FITC, 1ul CD45-APC Cytm7) and incubated in dark for 1.5-2h at 4°C according to the manufacturer's protocol. Cells (106 per unit) were subjected to flow cytometry (FACS) on a FACS Calibur and analyzed using FlowJo software. Three independent times of FACS were carried out for analysis.

Recombinant Adenovirus Vectors

Briefly, PCR-amplified mouse Wnt3a was subcloned into the vector pHBLV-CMV-EF1-RFP (Fig. 1) using the primer pair Wnt3a-EcoRI-F (5'acacgaattcATGGACAGAGCGGCGCTCC3') and Wnt3a-BamHI-R (5'acacggatccTTACTTACACGTGTGGACAT3'). The PCR products formed were confirmed by sequencing. The vector has been bought from HanBio company, Shanghai, China.

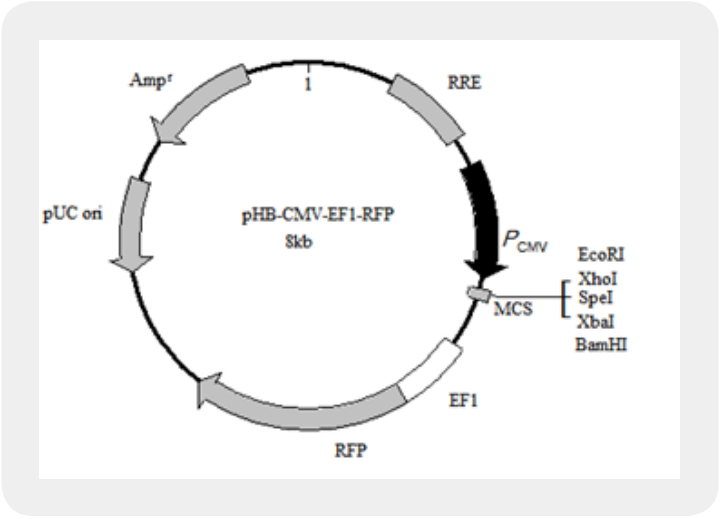

Figure 1: *The structure of the plasmid (pHBLV-CMV-EF1-RFP) for the Wnt3a expression vector.*

Lentivirus Packaging and Infection

HEK293T cells were cultured in DMEM with 10% FBS under a humid atmosphere containing 5% CO_2 at 37°C and reached 70-80% confluence for transfection. The target recombinant adenoviral plasmid and the auxiliary packaging original vector plasmid (pSPAX2 and pMD2G) were amplified in 293T cells by liposomes. After 48hrs transfection, the virus-containing medium was collected through the centrifuge of 72000g/min for 120min at 4°C. The supernatants contained wnt3a-GFP lentiviruses and GFP lentiviruses that infected periosteal cells at 37°C in CO2 incubator. The transfection efficiency of lentiviruses were detected by FACS.

The Effects of Wnt3a in Bone Information *in Vivo*

Wnt3a OE periosteal cells (107~108) were seeded on HA/TCP matrix (Wnt3a OE-cell-scaffold complex) and underwent subcutaneous transplantation on C57 mice (12-years-old, 25-30g weight, n=6). After two months transplantation, immunohistochemiscal staining, hematoxylin and eosin (H&E) staining and Masson trichrome staining were performed to evaluate the bone formation *in vivo*.

The Effects of Wnt3a in Bone Defect

Calvarial defect (5mm in diameter) mouse models (12-years-old, 25-30g weight) were established and randomly divided three groups: Wnt3a OE group (n=9), Control group (n=9), Blank group (n=9) and implanted with Wnt3a OE-cell-scaffold complex, cell-scaffold complex and scaffold respectively (10). After two months transplantation, the defected calvarial tissues were stained with H&E, Masson staining and scanned by micro-CT to evaluate the regeneration of bone defect. Fractional bone volume (bone volume per tissue volume, BV/TV), trabecular number (Tb.N), and separation (Tb.Sp) were calculated.

Statistical Analysis

All quantitative data were analyzed by SPSS Statistics (v.3a.0) and the significance of differences was determined using the ANOVA. Values are expressed as mean±SD with significance level set to $p<0.05$.

Results

The Generation of Wnt3a Over-Expressed Periosteal Cells

We harvested the periosteal cells from GFP mice and detected the mesenchymal stromal cell markers by FACS. 46.3% cells expressed CD105 positively and CD34 negatively, 50.6% cells expressed Sca-1 positively and CD45 negatively (Fig. 2). About 50% cells harvested from periosteum expressed both CD105 and Sca-1. For the lentiviruse transfection in GFP periosteal cells, about 22% population of periosteal cells were Wnt3a positive that were observed in yellow after overlap (Fig. 3). The FACS results further confirmed the over-expression of Wnt3a in Wnt3a positive cells (Fig. 4). The transfection rate was 22.1% that was consistent with the fluorescent microscope.

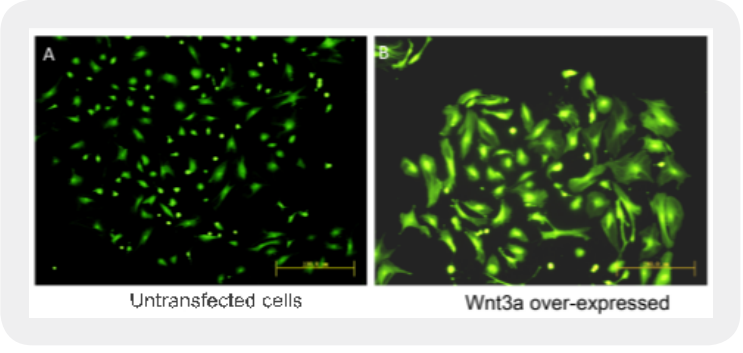

Figure 2: *The identification of Wnt3a over-expressed periosteal cells was detected by flow cytometry. A, Periosteal cells are negative in CD45 and positive in Sca-1; B: Periosteal cells are negative in CD34 and positive in CD105.*

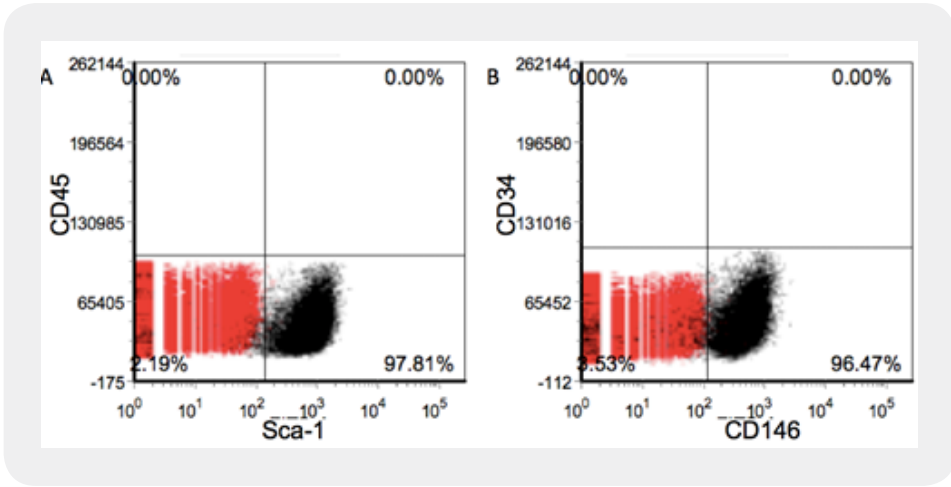

Figure 3: *Fluorescence microscopy showed the morphology and GFP positivity of periosteal cells. A. GFP periosteal cells are green; B. RFP Wnt3a OE periosteal cells are double stained with green and red that is yellow after overlap.*

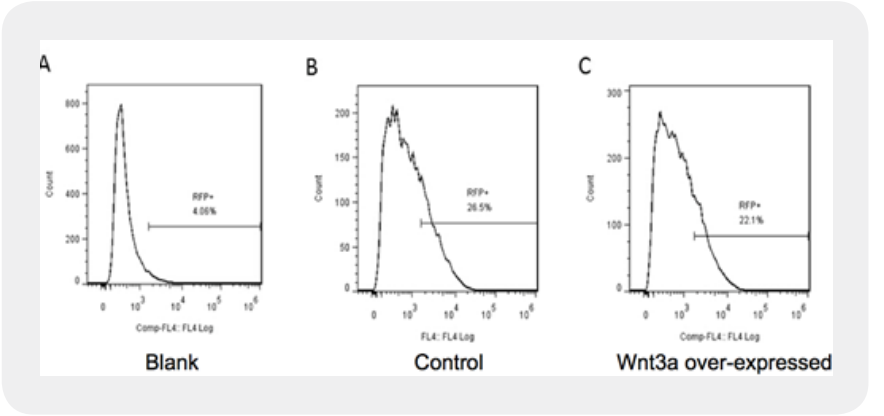

Figure 4: *Flow cytometry analyzed the Wnt3a OE of periosteal cells in protein level. A. Blank group; B. GFP periosteal cells; C. RFP Wnt3a OE periosteal cells.*

Wnt3a Promotes Atopic Bone Formation *in Vivo*

Wnt3a OE-cell-scaffold complex showed GFP positive after GFP immnunohistochemistry. Additionally, vessels, bone-like matrix and osteoblasts were observed in both complex after two-month implantation (Fig. 5). This suggested that periosteal cells and HA/TCP matrix promoted new bone formation *in vivo*. Compared to cell-scaffold complex, bone-like tissue was observed in Wnt3a OE-cell-scaffold complex and Wnt3a may enhance the osteogenesis of periosteal cells *in vivo*.

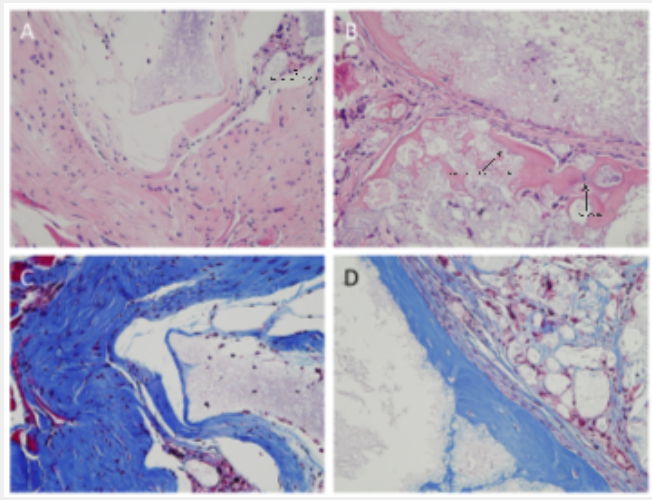

Figure 5: *H&E and Masson staining visualize the histology of the new bone. Control groups were stained with H&E staining, Masson staining (A, C). Wnt3a OE group were stained with H&E staining, Masson staining (B, D). Blood vessel, bone-like matrix and osteoblasts were labeled with arrows in H&E staining. Blue staining in Masson is collagen-like tissue and cartilage-like tissue. Red staining in Masson is cytoplasm and muscle tissue.*

Wnt3a Associates Bone Regeneration in Calvarial Defect

C57 mice were underwent calvarial defect operation and behaved normally before implantation [6]. Calvarial defect mice were transplanted with HA/TCP matrix, cell-scaffold complex, and Wnt3a OE-cell-scaffold complex. All the three groups were implanted for two-month and harvested for microtomography (Micro-CT) that provides structural or architectural information about a bone sample. For the coronal plane of Micro-CT analysis, Wnt3a OE group showed superior conjunction of new lamellar bone with the calvarial defect, compared with the other two groups (Fig 6). The length of connection is the longest in the Wnt3a OE group. In the blank group, the gap between new lamellar bone and calvarial defect is larger than the other two groups. For the vertical plane, the bone density is highest in Wnt3a OE group compared with the control and blank group (Fig 6). For the cross section analysis, yellow parts indicate the bone tissue and mineralization was identified in the grafted scaffold by Micro-CT. New bone formation occurred around the edge of the calvarical defect in all the three groups and only Wnt3a OE group showed new bone formation in the center of the defect area (Fig.6). Interestingly, bony islands were observed in the defect areas of the control and Wnt3a OE groups. Additionally, the volume of the new bone, the average space of bone trabecular, and the average number of bone trabecular were measured by Micro-CT system. Wnt3a OE group significantly generated higher volume, more bone trabecular and lower trabecular space in new bone, compared with those in the control and blank groups. (Fig 6). By contrast, the control group indicated no significant differences in the average space of bone trabecular and the average number of bone trabecular compared with the blank group.

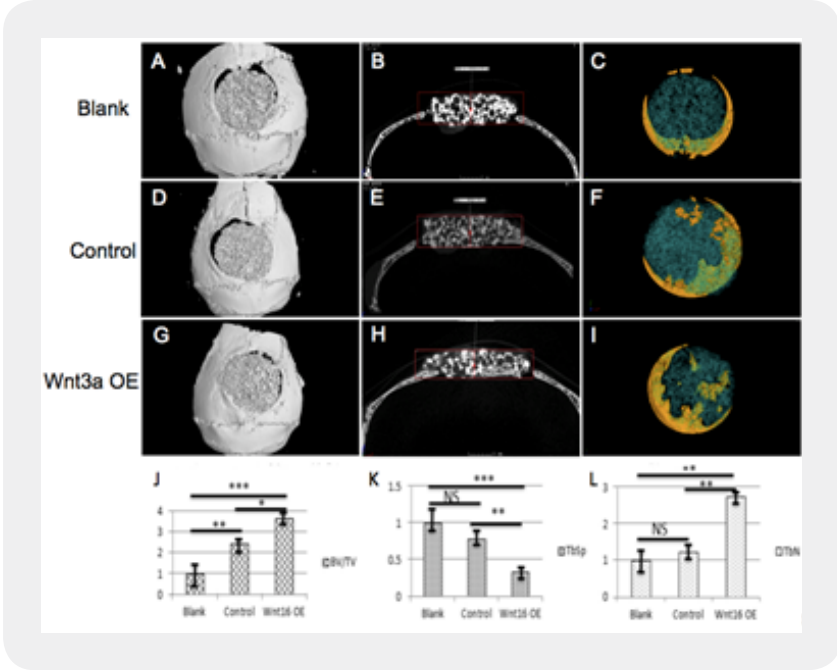

Figure 6: *Micro CT image of new bone formation in the calvarial defect. Calvarial defect was prepared and treated with HA/TCP (Blank group), the mix of HA/TCP and periosteal cells (Control group) and the mix of HA/TCP and Wnt3a OE periosteal cells (Wnt3a OE group), respectively. Micro CT images were undergone at 12 weeks after the surgery. Comparison of the micro-CT values in blank, control and Wnt3a OE group. The panels of A, D, G are the cross section of micro-CT image and the panels of B, E, F are the sagittal section of micro-CT image. The panels of C, E, F are the re-constructed 3D image. The volume of the new bone versus HA/TCP matrix (J), the average space of bone trabecular (K), and the average number of bone trabecular (L) were measured by micro-CT at 12 weeks after the surgery. Values are expressed as the mean ± S.E.M. for five animals in each group. * P<0.05, **P<0.01, ***P<0.005, NS means not statistically significant difference.*

Histological Analysis of New Bone in Calvarial Defect

Histological analysis were underwent further and included hematoxylin-eosin (H&E) staining and Massoon staining. H&E staining showed lamellar new bone formation were observed in the calvarial defect in the three groups (Fig.7 A, B, C). Wnt3a OE group showed the largest areas of lamellar new bone formation compared to the other two groups. Masson trichrome staining identifies muscle, collagen fibers, fibrin and erythrocytes (Fig.7 D, E, F). This was performed in the three groups that the results were consistent with H&E staining. In the aspect of vessel formation, Wnt 3a OE group and the control group had higher rate of new vessel formation.

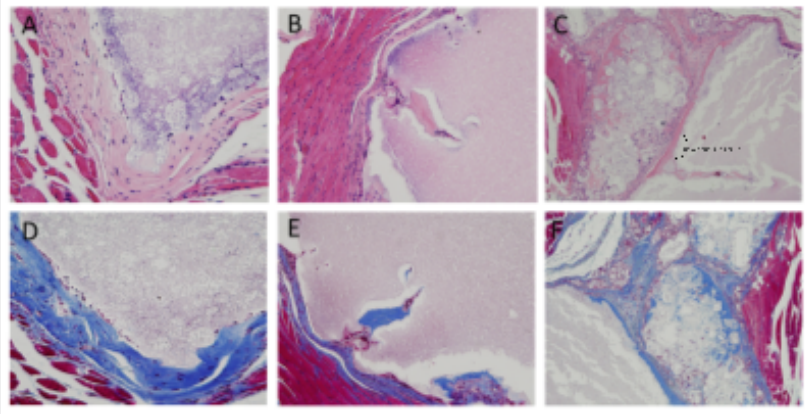

Figure 7: *New bone formation analyzed by histology. H&E and Masson trichrome staining were underwent at 12 weeks after the surgery. H&E staining was performed in in the blank (A), control (B) and Wnt3a OE group (C), respectively. Masson trichrome staining was performed in the blank (D), control (E) and Wnt3a OE group (F), respectively.*

Discussion

Wnt3a is one of the Wnt family members and has been involved in the regulation of osteogenesis [11]. Wnt proteins belongs to a family that secret cystein-rich glycoprotein and are regulated by Wnt canonical pathway (Wnt-β-catenin pathway) and noncanonical Wnt pathway [12,13]. Wnt3a has been reported in playing an important role in the cortical bone thickness and the risk of nonvertebal fracture in human beings. Wnt3a induced osteogenesis and inhibited osteoclastogenesis in mouse and human being. This modulated osteoclasts and promoted the osteoprotegerin (OPG) expression in osteoblasts [11]. Additionally, Wnt3a has been reported to be associated with bone mass and bone plasticity in a mouse model of osteogenesis imperfect [14]. In our study, Wnt3a has been involved in the osteogenesis of periosteum cells and *in vivo* bone defect regeneration model.

Wnt3a expression was upregulated in the perichondrium and periosteum in the development of skeleton [15]. Wnt3a was identified to be involved in the regulation of mouse craniofacial bone formation. Wnt3a expressed in the osteoid of calvaria, maxilla and mandible during intramembranous ossification. This process was between the expression of alkaline phophatase (ALP), osteocalcin (OCN) and the occurrence of bone mineralization [8]. Furthermore, the association between Wnt3a and bone mineral density (BMD), cortical bone thickness, bone strength and osteoporotic fracture risk has been proved by large population-based genome-wide association studies (GWASs) and in Wnt3a (Wnt3a-/-) knockout mouse model as well [16-18]. The deletion of Wnt3a caused cortical bone thickness and porosity and didn't affect trabecular bone mass. The up-regulation of Wnt3a promoted Opg expression in osteoblasts that contributed to inhibit osteoclastogenesis by suppressing RANKL-induced activation of nuclear factor-κB (NF-κB). It has been suggested that Wnt3a might act as a critical regulator for the communication between osteoblast and osteoclast in bone homeostasis [18]. In our study, we investigated the effects of Wnt3a involved in bone

formation *in vivo* by using mouse model and discovered that there were more vessels, bone-like matrix and osteoblasts observed in Wnt3a OE group, compared to control group. This suggested that Wnt3a might promote the osteogenic differentiation and contribute to the bone formation. We provide the evidence that Wnt3a might be also a key regulator in the promotion of osteogenesis. Additionally, other growth factors have also been reported in the involvement of bone formation. These factors include Vitamin K, basic fibroblast growth factor (bFGF), vascular endothelial growth factor (VEGF), stromal derivedgrowth factor-1alpha (SDF-1α), Insulin like growth factor-1 (Igf-1).

Nowadays clinical and socio-economic requirements are highlighted in the use of new bone to replace or maintain the function of damaged, traumatized or lost bone [2]. Tissue engineering and regenerative medicine shed a new light on the bone repair and regeneration. The discipline of tissue engineering in bone regeneration is in the combination of cells with scaffolds, or with growth factors, by which initiates and promotes osteogenesis. In the study, we used periostem cells, osteo-inducible scaffolds, and biological factor Wnt3a to create a robust and biocompatible bone regeneration strategies to repair the bone defect. This is targeted to address the requirement for bone regeneration and skeletal repair.

In this study, we choose the mouse calvarial defect model for the study of bone regeneration, which is a convenient model and has less risk in the occurrence of complication [19]. A 5-mm calvarial bone defect has been considered as a critical-size defect and the application of the HA/TCP scaffold not only provided with physical support but also extracellular microenvironment. As a supportive platform, the material scaffold has advantage and disadvantage, which is analysis along with various architectural parameters, including interconnectivity, porosity, pore size and pore-wall microstructures [1].

After two months of implantation, all the calvarial defect mice were investigated by both Micro CT and histological analysis, which were used widely and reliable in the assessment of bone regeneration [20]. Micro CT showed that new bone formation in the defect border was observed between the implanted sites and the host bone in all the three groups. In the blank group, the proliferation of host bone cells and the physical support of the scaffold contributed to the new bone formation. In the control group, the periostem cells divided into osteoblast and more volume of trabecular bone were regenerated compared to the blank group. Interestingly, new bone was regenerated into deeper parts of the scaffold and bony islands scattered in the defect areas in the Wnt 3a OE group. This indicated Wnt3a derive osteoblast *in vivo* [21]. In our study, Masson trichrome staining demonstrated that a larger number of vascular blood formation in the control and Wnt3a OE groups, which resulted from the combination of the scaffold with periostem cells (Fig.5 C, D). The establishment of a vessel blood network is the key of tissue engineering. The vasculogenesis and angiogenesis are provided with nutrition supply, gaseous exchange and waste removal during the new bone formation [2,22-24].

Conclusions

The results of this study indicated that the use of periostem cells enhanced bone defect regeneration and the Wnt3a OE promoted bone formation and mineralization. Moreover, the establishment of blood vessel network was also observed. The combination with the HA/TCP scaffold and Wnt3a provided a osteogenesis-like microenvironment, which promoted the bone repair and regeneration in the calvarial defect *in vivo*.

Acknowledgements

The authors declare that there is no conflict of interest regarding the publication of this paper.

Bibliography

1. Hutmacher, D. W., Schantz, J. T., Lam, C. X. F., Tan, K. C. & Lim, T. C. (2007). State of the art and future directions of scaffold-based bone engineering from a biomaterials perspective. *Journal of Tissue Engineering and Regenerative Medicine, 1*(4), 245-260.

2. Woodruff, M. A., Lange, C., Reichert, J., Berner, A., Chen, F., Fratzl, P., *et al.* (2012). Bone tissue engineering: from bench to bedside. *Materials Today, 15*(10), 430-435.

3. Dwek, J. R. (2010). The periosteum: what is it, where is it, and what mimics it in its absence? *Skeletal Radiology, 39*(4), 319-323.

4. Hoffman, M. D. & Benoit, D. S. (2015). Emulating native periosteum cell population and subsequent paracrine factor production to promote tissue engineered periosteum-mediated allograft healing. *Biomaterials, 52,* 426-440.

5. Roberts, S. J., van Gastel, N., Carmeliet, G. & Luyten, F. P. (2015). Uncovering the periosteum for skeletal regeneration: The stem cell that lies beneath. *Bone, 70,* 10-18.

6. Vamze, J., Pilmane, M. & Skagers, A. (2015). Biocompatibility of pure and mixed hydroxyapatite and alpha-tricalcium phosphate implanted in rabbit bone. *Journal of Materials Science Materials in Medicine, 26*(2), 73.

7. Rojbani, H., Nyan, M., Ohya, K. & Kasugai, S. (2011). Evaluation of the osteoconductivity of alpha-tricalcium phosphate, beta-tricalcium phosphate, and hydroxyapatite combined with or without simvastatin in rat calvarial defect. *Journal of Biomedical Materials Research Part A, 98*(4), 488-498.

8. Jiang, Z., Von den Hoff, J. W., Torensma, R., Meng, L. & Bian, Z. (2014). Wnt16 is involved in intramembranous ossification and suppresses osteoblast differentiation through the Wnt/beta-catenin pathway. *Journal of Cellular Physiology, 229*(3), 384-392.

9. Moverare-Skrtic, S., Henning, P., Liu, X., Nagano, K., Saito, H., Borjesson, A. E., *et al.* (2014). Osteoblast-derived WNT16 represses osteoclastogenesis and prevents cortical bone fragility fractures. *Nature Medicine, 20*(11), 1279-1288.

10. Guo, X., Day, T. F., Jiang, X., Garrett-Beal, L., Topol, L. & Yang, Y. (2004). Wnt/beta-catenin signaling is sufficient and necessary for synovial joint formation. *Genes & Development, 18*(19), 2404-2417.

11. Song, J., McColl, J., Camp, E., Kennerley, N., Mok, G. F., McCormick, D., *et al.* (2014). Smad1 transcription factor integrates BMP2 and Wnt3a signals in migrating cardiac progenitor cells. *Proceedings of the National Academy of Sciences of the United States of America, 111*(20), 7337-7342.

12. Baron, R. & Kneissel, M. (2013). WNT signaling in bone homeostasis and disease: from human mutations to treatments. *Nature Medicine, 19*(2), 179-192.

13. Cadigan, K. M. & Peifer, M. (2009). Wnt signaling from development to disease: insights from model systems. *Cold Spring Harbor Perspectives in Biology, 1*(2), a002881.

14. Belinsky, G. S., Sreekumar, B., Andrejecsk, J. W., Saltzman, W. M., Gong, J., Herzog, R. I., *et al.* (2016). Pigment epithelium-derived factor restoration increases bone mass and improves bone plasticity in a model of osteogenesis imperfecta type VI via Wnt3a blockade. *Federation of American Societies for Experimental Biology, 30*(8), 2837-2848.

15. Witte, F., Dokas, J., Neuendorf, F., Mundlos, S. & Stricker, S. (2009). Comprehensive expression analysis of all Wnt genes and their major secreted antagonists during mouse limb development and cartilage differentiation. *Gene Expression Patterns: GEP., 9*(4), 215-223.

16. Zheng, H. F., Tobias, J. H., Duncan, E., Evans, D. M., Eriksson, J., Paternoster, L., *et al.* (2012). WNT16 influences bone mineral density, cortical bone thickness, bone strength, and osteoporotic fracture risk. *PLoS Genetics., 8*(7), e1002745.

17. Movérare-Skrtic, S., Henning, P., Liu, X., Nagano, K., Saito, H., Börjesson, A. E., *et al.* (2014). Osteoblast-derived WNT16 represses osteoclastogenesis and prevents cortical bone fragility fractures. *Nature Medicine, 20*(11), 1279-1288.

18. Gori, F., Lerner, U., Ohlsson, C. & Baron, R. (2015). A new WNT on the bone: WNT16, cortical bone thickness, porosity and fractures. *BoneKEy Reports, 4,* 669.

19. Verna, C., Dalstra, M., Wikesjö, U. M. & Trombelli, L. (2002). Healing patterns in calvarial bone defects following guided bone regeneration in rats. *Journal of Clinical Periodontology, 29*(9), 865-870.

20. Asutay, F., Polat, S., Gül, M., Subaşı, C., Kahraman, S. A. & Karaöz, E. (2015). The effects of dental pulp stem cells on bone regeneration in rat calvarial defect model: Micro-computed tomography and histomorphometric analysis. *Archives of Oral Biology, 60*(12), 1729-1735.

21. Thuaksuban, N., Nuntanaranont, T., Suttapreyasri, S. & Boonyaphiphat, P. (2015). Repairing calvarial defects with biodegradable polycaprolactone-chitosan scaffolds fabricated using the melt stretching and multilayer deposition technique. *Bio-Medical Materials and Engineering, 25*(4), 347-360.

22. Stegen, S., van Gastel, N. & Carmeliet, G. (2015). Bringing new life to damaged bone: The importance of angiogenesis in bone repair and regeneration. *Bone, 70,* 19-27.

23. Mamalis, A. A. & Cochran, D. L. (2011). The therapeutic potential of oxygen tension manipulation via hypoxia inducible factors and mimicking agents in guided bone regeneration. A review. *Archives of Oral Biology, 56*(12), 1466-1475.

24. Almubarak, S., Nethercott, H., Freeberg, M., Beaudon, C., Jha, A., Jackson, W., *et al.* (2015). Tissue engineering strategies for promoting vascularized bone regeneration. *Bone, 83,* 197-209.